ChemPubSoc Europe

DOI: 10.1002/cmdc.201500288

CHEMMEDCHEM Full Papers

Phototoxic Activity and DNA Interactions of Water-Soluble Porphyrins and Their Rhenium(I) Conjugates

Giuliana Mion,[a] Teresa Gianferrara,*[a] Alberta Bergamo,[b] Gilles Gasser,*[c] Vanessa Pierroz,[c] Riccardo Rubbiani,[c] Ramon Vilar,*[d] Anna Leczkowska,[d] and Enzo Alessio[a]

In the search for alternative photosensitizers for use in photodynamic therapy (PDT), herein we describe two new water-soluble porphyrins, a neutral fourfold-symmetric compound and a +3-charged tris-methylpyridinium derivative, in which either four or one [1,4,7]-triazacyclononane (TACN) units are connected to the porphyrin macrocycle through a hydrophilic linker; we also report their corresponding tetracationic Re^{I} conjugates. The in vitro (photo)toxic effects of the compounds toward the human cell lines HeLa (cervical cancer), H460M2 (non-small-cell lung carcinoma), and HBL-100 (non-tumorigenic epithelial cells) are reported. Three of the compounds are not cytotoxic in the dark up to 100 μM, and the fourfold-symmetric couple revealed very good phototoxic indexes (PIs). The intracellular localization of all derivatives was studied in HeLa cells by confocal fluorescence microscopy. Although low nuclear localization was observed for some of them, it still prompted us to investigate their capacity to bind both quadruplex and duplex DNA; we observed significant selectivity in the tris-methylpyridinium derivatives for G-quadruplex interactions.

Introduction

Photodynamic therapy (PDT) is emerging as a particularly attractive clinical method to treat cancers, infectious diseases, and a series of local afflictions.[1–4] This therapeutic strategy is an alternative or adjuvant to other therapy modalities such as surgery, chemotherapy, or radiotherapy.[5] The basic principle of PDT is the light-mediated activation of a nontoxic tumor-localized photosensitizer (PS). Thus, upon irradiation at a specific desired wavelength, the PS reaches an excited triplet state (PS*). PS* can transfer electrons or protons to substrates in close proximity, giving rise to radical anions or cations, respectively, that are subsequently scavenged by oxygen to form reactive oxygen species (ROS, type I mechanism). As an alternative, PS* can transfer its energy directly to the ground state of the molecular triplet oxygen ($^3O_2$) to form singlet oxygen ($^1O_2$, type II mechanism), a very reactive and toxic form of oxygen. $^1O_2$ is believed to be the major cytotoxic agent in PDT. It is able to induce cell death by apoptosis and necrosis, immunological effects, vascular shutdown, and can trigger inflammatory responses.[6–10] As a consequence of its high reactivity, $^1O_2$ has a short lifetime in the physiological environment, and its action occurs close to the site of formation within the cell.[11–13] Therefore, besides being typically noninvasive (e.g., relative to surgery),[14–17] PDT treatment offers several advantages over current cancer treatments, namely: 1) the possibility to induce cell death with precise spatial and temporal control, 2) low systemic toxicity, as the cytotoxic effects are triggered only in selectively irradiated tissues,[18] 3) the possibility to be repeated several times at the same site, and 4) the possibility to exploit the inherent fluorescence properties of PSs in photodynamic diagnosis (PDD).[19,20]

The most frequently used PSs in PDT are porphyrins and porphyrinoids, because they preferentially accumulate in tumor tissues and are efficient singlet oxygen generators.[2,21,22] There has been a recent growth in interest in the preparation of metal–porphyrin conjugates as potential cytotoxic and photocytotoxic agents. Such conjugates might combine the phototoxicity of the porphyrin chromophore with the cytotoxicity of the metal fragment for additive antitumor effects. In addition, these conjugates might have increased tumor selectivity. The first metal–porphyrin conjugates developed for biomedical applications were porphyrins functionalized with Pt^{II} fragments structurally related to cisplatin and carboplatin.[23–26] More recent examples concern several Ru^{II}–porphyrin conjugates developed in particular by some of us,[27] and by Therrien and coworkers,[28,29] that possess promising phototoxicity induced by visible light. Furthermore, the water solubility of the porphyrins can be considerably improved by an appropriate choice of the peripheral metal fragments. This is an essential feature for clinical application; indeed, the low water solubility of synthet-

[a] G. Mion, Dr. T. Gianferrara, Prof. E. Alessio
Department of Chemical & Pharmaceutical Sciences
Università degli Studi di Trieste, P.le Europa 1, 34127 Trieste (Italy)
E-mail: gianfer@units.it

[b] Dr. A. Bergamo
Callerio Foundation Onlus, Via A. Fleming 22–31, 34127 Trieste (Italy)

[c] Prof. G. Gasser, Dr. V. Pierroz, Dr. R. Rubbiani
Department of Chemistry, University of Zurich
Winterthurerstrasse 190, 8057 Zurich (Switzerland)
E-mail: gilles.gasser@chem.uzh.ch

[d] Prof. R. Vilar, Dr. A. Leczkowska
Department of Chemistry, Imperial College London, London SW7 2AZ (UK)
E-mail: r.vilar@imperial.ac.uk

Supporting information for this article is available on the WWW under http://dx.doi.org/10.1002/cmdc.201500288.

ic porphyrins is a substantial limitation, as it may impair both their administration and efficacy.

More recently, we described the preparation and characterization of two novel water-soluble porphyrins bearing three *meso*-pyridyl rings and one peripheral chelator, which was either a diethylenetriamine unit or a bipyridyl fragment. Both chelators were suitable for complexation of the $\{^{99m}Tc/Re(CO)_3\}^+$ moieties.[30,31] Technetium is the most widely used radionuclide in diagnosis, and rhenium is its heavier homologue. The properties of the "cold" Re and of the "hot" ^{99m}Tc complexes are assumed to be very similar. By applying the matched pair paradigm, the $Re^I/^{99m}Tc^I$–porphyrin conjugates may act as multifunctional agents endowed either with diagnostic (^{99m}Tc) or with therapeutic properties (Re).[32] In principle, radioimaging performed on a labeled $^{99m}Tc^I$–porphyrin might allow noninvasive, in vivo localization of the corresponding PDT active "cold" Re conjugate.

Whereas metal complexes based on platinum and ruthenium have been studied extensively as anticancer agents, relatively few rhenium complexes have been explored as potential anticancer agents, although they possess excellent properties for developing a novel class of antineoplastic drug.[33,34] Notably, certain organometallic rhenium complexes have been found to have interesting luminescence properties which allow their intracellular distribution as well as their mechanism of action to be followed by emission microscopy.[35] But the most attractive property of Re compounds is the possibility to obtain the corresponding "hot" analogues, suitable for therapy, by using ^{186}Re and ^{188}Re radionuclides.

The ability of cationic porphyrins and their metal complexes to interact with nucleic acids is well documented,[26,36] and one of the most extensively investigated compounds is *meso*-tetrakis-(4-*N*-methylpyridiniumyl)porphyrin (TMPyP). The original work of Fiel and co-workers on the interactions of TMPyP with DNA was aimed at developing DNA-targeting photosensitizers, as selective photocleavage of DNA in tumor cells might result in lethal damage to the cells.[36a,37] Furthermore, cationic porphyrins were recently exploited for selective recognition of noncanonical DNA structures called G-quadruplexes.[38–42] The formation of G-quadruplex DNA structures in vivo has been associated with a number of key biological processes such as regulation of gene expression and telomere maintenance. In general, cationic porphyrins with relatively long and flexible side arms are better binders of G-quartets than TMPyP4, presumably because they might permit stacking of the aromatic porphyrin core on the G-tetrad, minimizing steric clashes with the G-tetrad edges.[40] Furthermore, there is mounting interest in synthetizing cationic asymmetric porphyrins as G-quadruplex ligands, in particular to obtain molecules endowed with an increased overall affinity for the telomeric structures by virtue of additional interactions.[43] Due to the important biological roles associated to G-quadruplexes, they are potential targets for anticancer drug candidates.[44] Furthermore, it is well known that DNA can be damaged by exogenous and endogenous oxidative stress induced by reactive oxygen (ROS) and nitrogen species (RNS). ROS include superoxide anion radical ($O_2^{-\bullet}$), hydrogen peroxide (H_2O_2), hydroxyl radicals ($OH^{-\bullet}$) and singlet oxygen ($^1O_2$). These species can oxidize purine and pyrimidine bases, damage the DNA at apurinic/apyrimidinic (abasic) sites, and can also give rise to single-strand (SSBs) and double-strand breaks (DSBs).[45]

For all the reasons detailed above, we decided to investigate tetrapyrrolic chromophores suitable for conjugation with Re fragments to be used in both therapy and diagnosis of cancer. Herein we describe the synthesis, characterization, cellular localization, evaluation of the affinity for both quadruplex and duplex DNA, and (photo)toxic behavior of two novel porphyrins functionalized with either four or one [1,4,7]-triazacyclononane (TACN) peripheral units—the neutral **1** and the +3-charged **3**—as well as of their corresponding tetracationic Re^I conjugates **2** and **4** (Figure 1). Porphyrins **1** and **3** were specifically designed for binding a facial metal fragment such as $Re/Tc(CO)_3$. In fact, the neutral TACN chelating unit matches the binding preferences of those metal fragments, providing a relatively rigid set of three thermodynamically and kinetically stable bonds. Hence, **1** and **3** are an evolution of two monofunctionalized porphyrins previously synthesized by us, which bear a bidentate (bypyridyl) or tridentate (diethylenetriamine) ligand, respectively (Figure 2a,c).[30,31] Of note, the open-chain diethylenetriamine ligand has a poorer geometrical match than TACN and, being flexible, is a less efficient binder than TACN. The bidentate bipyridyl ligand is hydrophobic and leaves a hydrolysable position upon coordination with the $Re/Tc(CO)_3$ fragment (Figure 2d). The coordination chemistry of Re^I/Tc^I with TACN as a ligand is well documented, and a variety of complexes containing rhenium, as well as technetium, in the formal oxidation state I+ with TACN have been reported.[46–48]

Results and Discussion

Synthesis and characterization

Porphyrins **1** and **3** bear four or one TACN ligands, respectively, which are attached at phenyl rings at the *meso* positions (Figure 1). To prepare them, a suitably functionalized TACN derivative, 2-(diBoc)TACN acetic acid (**5**), was synthesized in good yield by selective 1,4-diprotection of the amino groups of TACN,[49] followed by reaction with benzyl bromoacetate and reductive deprotection with H_2 on Pd/C (Supporting Information Scheme S1). The synthetic procedures to obtain **1** and **3** start from two precursors that bear either four (**6**, Scheme 1) or one (**8**, Scheme 2) hydrophilic 2,2′-(ethylenedioxy)diethylamine chains on *meso*-phenyl rings (*para* position) on the macrocycles. The multistep syntheses of **6** and **8** were described previously.[27,30] The hydroxybenzotriazole (HOBt) ester of **5** was then coupled with the terminal amino group of either **6** or **8** in anhydrous DMF to give **7** (66% yield) and **9** (66% yield), respectively. These intermediates were quantitatively deprotected using trifluoroacetic acid (TFA) in CH_2Cl_2, and treated with triethylamine (TEA) to give the neutral tetrafunctionalized porphyrin **1** or the +3-charged monofunctionalized porphyrin **3**, respectively. Both porphyrins were characterized by UV/Vis, ^1H NMR, H–H COSY, HSQC spectroscopy, electrospray mass

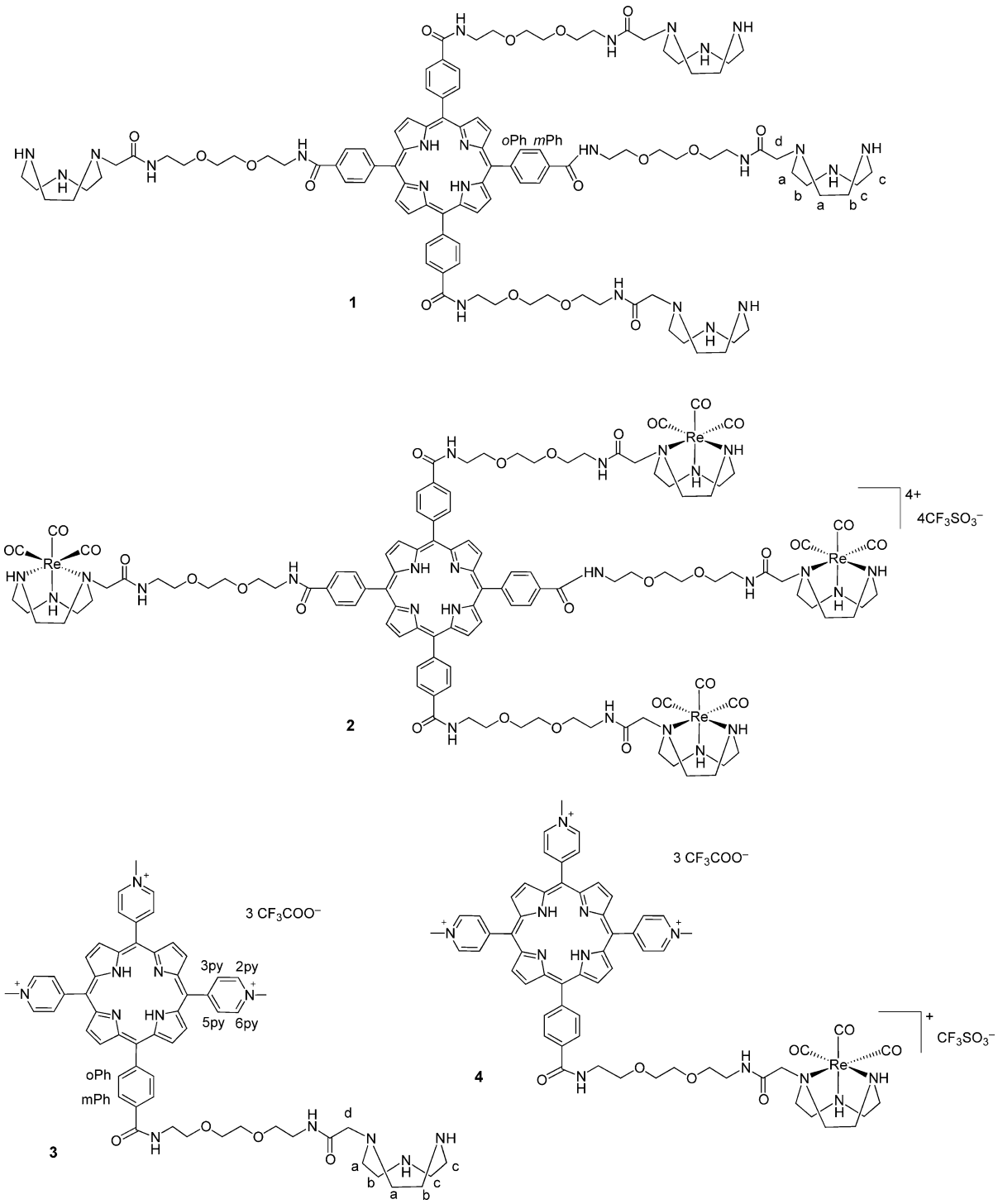

Figure 1. Structures of porphyrins and Re–porphyrin conjugates **1**–**4** used in this study with NMR labeling scheme.

spectrometry (Figures S3, S4, S8, and S9 in the Supporting Information), and by ESI HRMS, and were found to be well soluble in water.

The TACN moieties provide three N atoms in facial geometry, and are thus particularly well suited for binding the *fac*-$\{Re(CO)_3\}^+$ fragment. To obtain the corresponding rhenium conjugates, **2** and **4** (Figure 1), each porphyrin was reacted with the Re^I precursor *fac*-$[Re(CO)_3(dmso\text{-}O)_3](CF_3SO_3)$. Whereas **2** was obtained by holding the starting materials at reflux in anhydrous methanol (60% yield; Scheme 1), a microwave reaction at 110 °C in methanol was necessary to afford conjugate **4** in good yield (73%; Scheme 2). Both reactions were monitored by TLC and by recording ^1H NMR spectra of the reaction mixtures at time intervals (Figures S5 and S14, Supporting Informa-

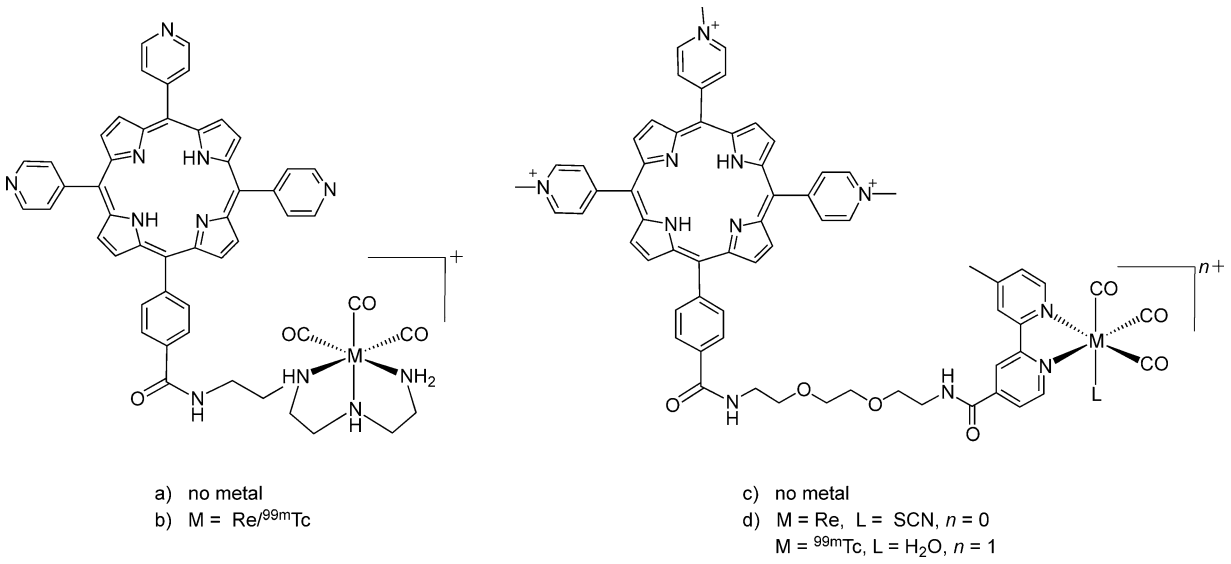

Figure 2. Structures of previously described Re/^{99m}Tc–porphyrin conjugates.[30,31]

tion). The resonances of Hd and NH of TACN (see Figure 1 for labeling scheme) move significantly downfield upon Re coordination, and are thus diagnostic of product formation.

Notably, upon coordination of **1** and **3** to the *fac*-{Re(CO)$_3$}$^+$ fragment, both conjugates become tetracationic. The rhenium conjugates **2** and **4** were characterized by one- and two-dimensional NMR (Figures S6 and S7, Figures S10–13, Supporting Information) and IR spectroscopy. All compounds are well (**1**, **3**, and **4**), or at least appreciably (**2**), soluble in water, besides being soluble in DMSO.

(Photo)toxicity studies

The (photo)toxic activity of compounds **1**–**4** was assessed on three different cell lines, namely the cervical cancer cell line HeLa, the lung cancer cell line H460M2, and the non-tumorigenic cell line HBL-100. Effects on cell growth were evaluated both in the dark and upon irradiation with red light ($\lambda =$ 650 nm) for each compound. Cell cultures were exposed for 24 h at concentrations ranging from 0.1 to 100 μM, and were then irradiated with a fluence rate of 14 mW cm^{-2} and light doses from 1 to 10 J cm^{-2}. As a control, we could show that the light doses used in this study do not influence the proliferation of untreated cells. Cells treated with the same concentrations of test compounds and kept in the dark were used as controls for phototoxicity. The (photo)toxicity of compounds **1**–**4** against the selected cell lines at increasing total light doses is reported in Table 1.

The phototoxicity of compounds **1** and **2** was found to increase upon to the total light dose used, as shown by the dose–effect curves on HeLa and H460M2 cells (Figure 3). By irradiating tumor cells at increasing total light doses from 1 to 10 J cm^{-2}, the dose–response curve shifts to the left, and the IC$_{50}$ value correspondingly decreases.

All compounds were found to be non-cytotoxic in the dark, with the exception of **2**, which proved to be cytotoxic toward both H460M2 and HBL-100 cell lines, with IC$_{50}$ values of 7.4 and 33.7 μM, respectively, but not toward HeLa cells at the maximum concentration used. This result is consistent with observations reported previously[27,50,51] that tetrasubstituted porphyrin–Ru^{II} conjugates typically show remarkable cytotoxicity in the absence of light. The negligible dark cytotoxicity of the Re^{I} conjugates **4** is consistent with what was found for monosubstituted porphyrin–Ru^{II} conjugates by several research groups.[51–53] After exposure to red light, the monofunctionalized compounds **3** and **4** were consistently less active than the tetrafunctionalized compounds **1** and **2** under the same experimental conditions used for determining phototoxicity. In particular, compounds **3** and **4** are not effective at the lowest light dose (1 J cm^{-2}) on all the cell lines (IC$_{50}$ values $>$100 μM). Instead, an activity from mild to moderate was always observed at 10 J cm^{-2}, with a greater effectiveness of both porphyrins against the H460M2 tumor cell line (IC$_{50}$: 13 and 12 μM for **3** and **4**, respectively).

A comparison between compounds **1** and **2** reveals a greater phototoxic effect of the latter against the HeLa cell line at all light doses (e.g., PI at 10 J cm^{-2} $>$7.8 and $>$71.4, respectively, Table 1). Conjugate **2** showed a PI value of $>$38.5 upon irradiation at 5 J cm^{-2}, which is consistent with the PIs of known PSs, photofrin and hypericin[21] ($>$10 and $>$43, respectively, at the same light dose).[54] However, under the same experimental conditions, a much higher PI ($>$200) was determined for the porphyrin bearing a diethylenetriamine ligand (Figure 2a). On the other hand, porphyrin **1** is $>$77-fold more active after irradiation at 10 J cm^{-2} on H460M2 cells, whereas **2** has a much lower PI ($>$14.8, both at 5 and 10 J cm^{-2}, Table 1). The cytotoxicity of conjugate **2** on H460M2 cells in the dark, with an IC$_{50}$ value very close to that found after photo-irradiation, indicates a different sensitivity between the two cell lines. These results suggest that the Re–porphyrin conjugate **2** is not suitable for non-small-cell lung cancers. However, it could be used in PDT for cervical cancer and other tumor types that similarly show

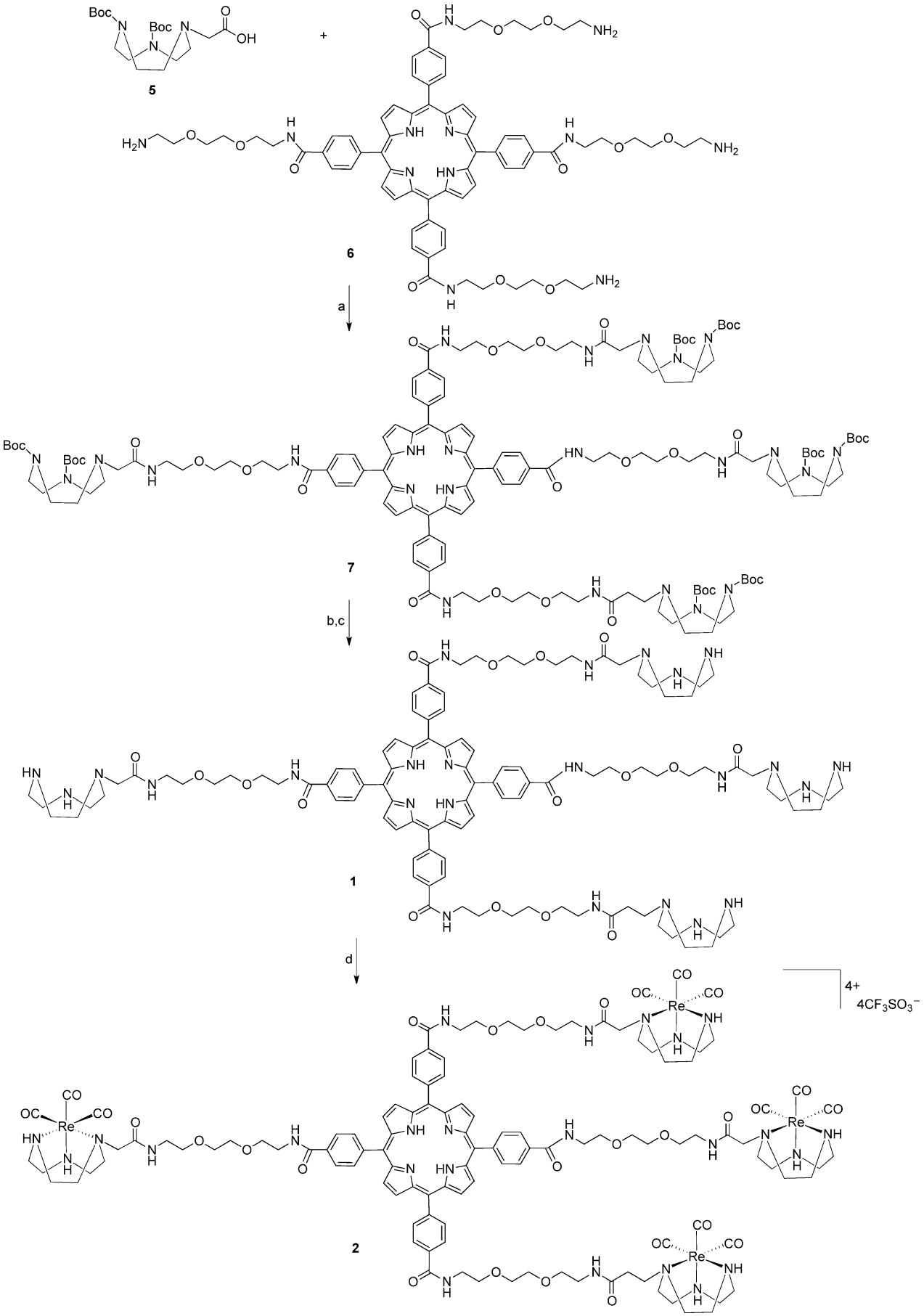

Scheme 1. Synthetic route to **1** and **2**. *Reagents and conditions*: a) DMAP, EDCI, HOBt, DMF, 24 h, RT, 66%; b) CH_2Cl_2, TFA, 3 h, RT; c) CH_3OH, TEA, Et_2O, 97%; d) *fac*-$[Re(CO)_3(dmso\text{-}O)_3](CF_3SO_3)$, anhydrous CH_3OH, 48 h, 70 °C, reflux, 65%.

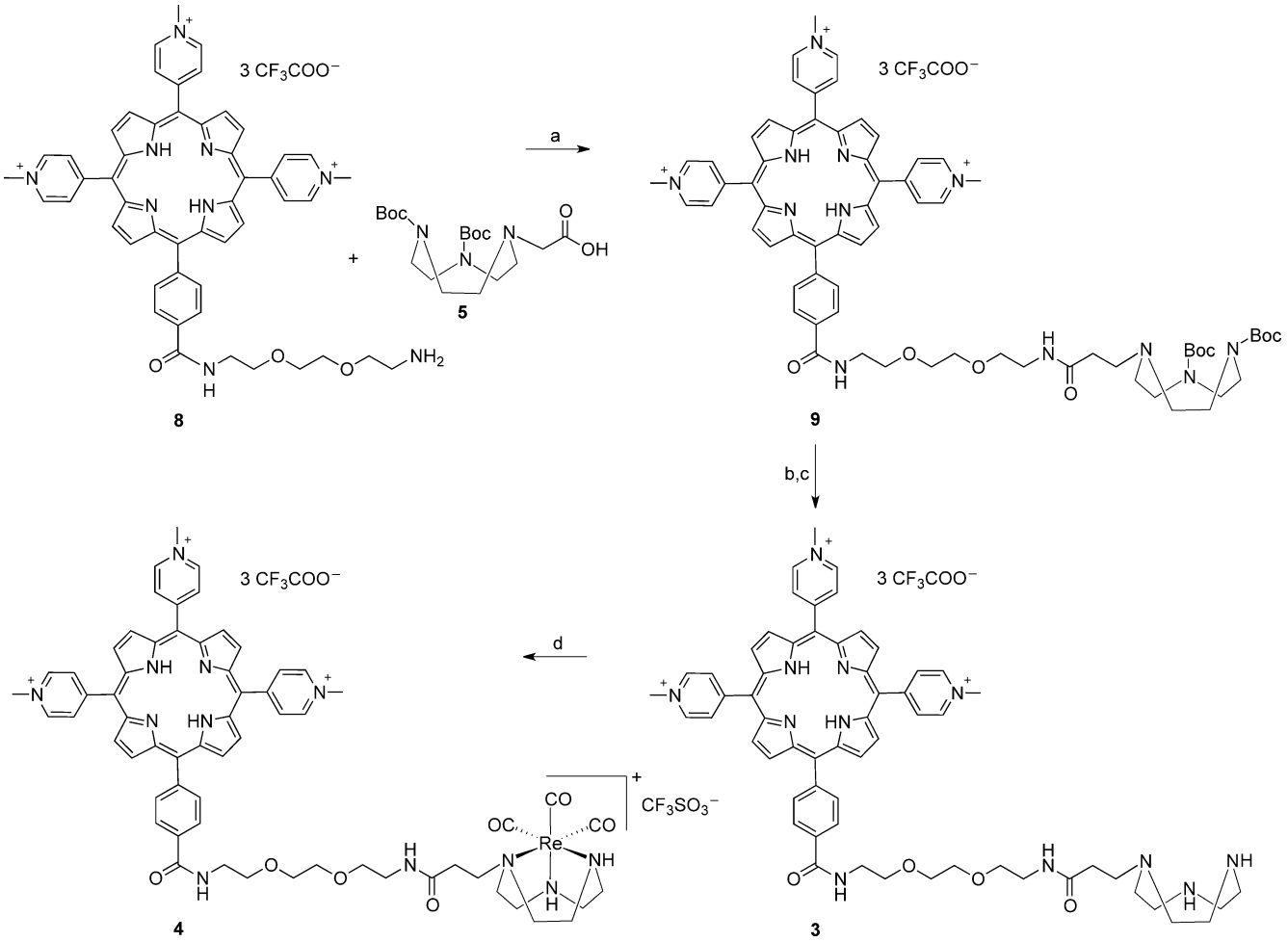

Scheme 2. Synthetic route to **3** and **4**. *Reagents and conditions*: a) DMAP, EDCI, HOBt, DMF, MW 6 min, 60 °C, 66%; b) TFA, CH_2Cl_2, 3 h, RT; c) TEA, CH_3OH/Et_2O, 98%; d) *fac*-$[Re(CO)_3(dmso\text{-}O)_3](CF_3SO_3)$, CH_3OH, MW 10 min, 110 °C, 73%.

Table 1. IC_{50} [μM] values and phototoxic indexes (PI) in HeLa, H460M2, and HBL-100 cells treated for 24 h with compounds **1**–**4** (0.1, 1, 3, 10, 30, and 100 μM) and then exposed to increasing doses of red light ($\lambda = 650$ nm).[a]

Cell line	Compd	Dark	1 J cm^{-2}	PI[b]	5 J cm^{-2}	PI[b]	10 J cm^{-2}	PI[b]
HeLa	**1**	>100	>100	ND[c]	>100	ND[c]	12.9±3.0	>7.8
	2	>100	32.6±4.4	>3	2.6±1.6	>38.5	1.4±1.3	>71.4
	3	>100	>100	ND[c]	>100	ND[c]	100±41	>1
	4	>100	>100	ND[c]	≥100	ND[c]	73±19	>1.4
H460M2	**1**	>100	35.5±7.7	>2.8	4.3±1.3	>23.3	1.3±0.6	>77
	2	7.4±2.0	2.8±1.4	>2.6	0.5±0.2	>14.8	0.5±0.2	>14.8
	3	>100	>100	ND[c]	≥100	ND[c]	13±1	>7.7
	4	>100	>100	ND[c]	58±9	>1.7	12±5	>8.3
HBL-100	**1**	>100	82.0±7.4	>1.2	4.8±2.9	>20.8	1.4±0.9	>71.4
	2	33.7±14.5	9.4±3.4	>3.6	1.0±0.3	>33.7	0.5±0.1	>67.4
	3	>100	>100	ND[c]	76.6±1.6	>1.3	23.4±12.0	>4.3
	4	>100	>100	ND[c]	75.4±0.1	>1.3	42.8±5.3	>2.3

[a] Cells were exposed for 24 h to each compound at concentrations ranging from 0.1 to 100 μM. Cells were then irradiated at $\lambda = 650$ nm with a fluence rate of 14 mW cm^{-2} for increasing time intervals (71 s; 5 min, 57 s; 11 min, 54 s) corresponding to total light doses of 1, 5, or 10 J cm^{-2}. These light doses do not affect proliferation of untreated cells in control experiments. Cell cytotoxicity was determined by MTT assay 24 h post-irradiation. Cells treated with the same concentrations of the test compounds, but kept in the dark, were used as controls. IC_{50} values were calculated from dose–effect curves and are the mean ±SD of at least three separate experiments. Experiments were conducted in quadruplicate and repeated thrice. Statistical analyses (not reported in the table): ANOVA and Tukey–Kramer post-test. [b] PI = IC_{50} in the dark/IC_{50} upon irradiation. [c] Not determinable.

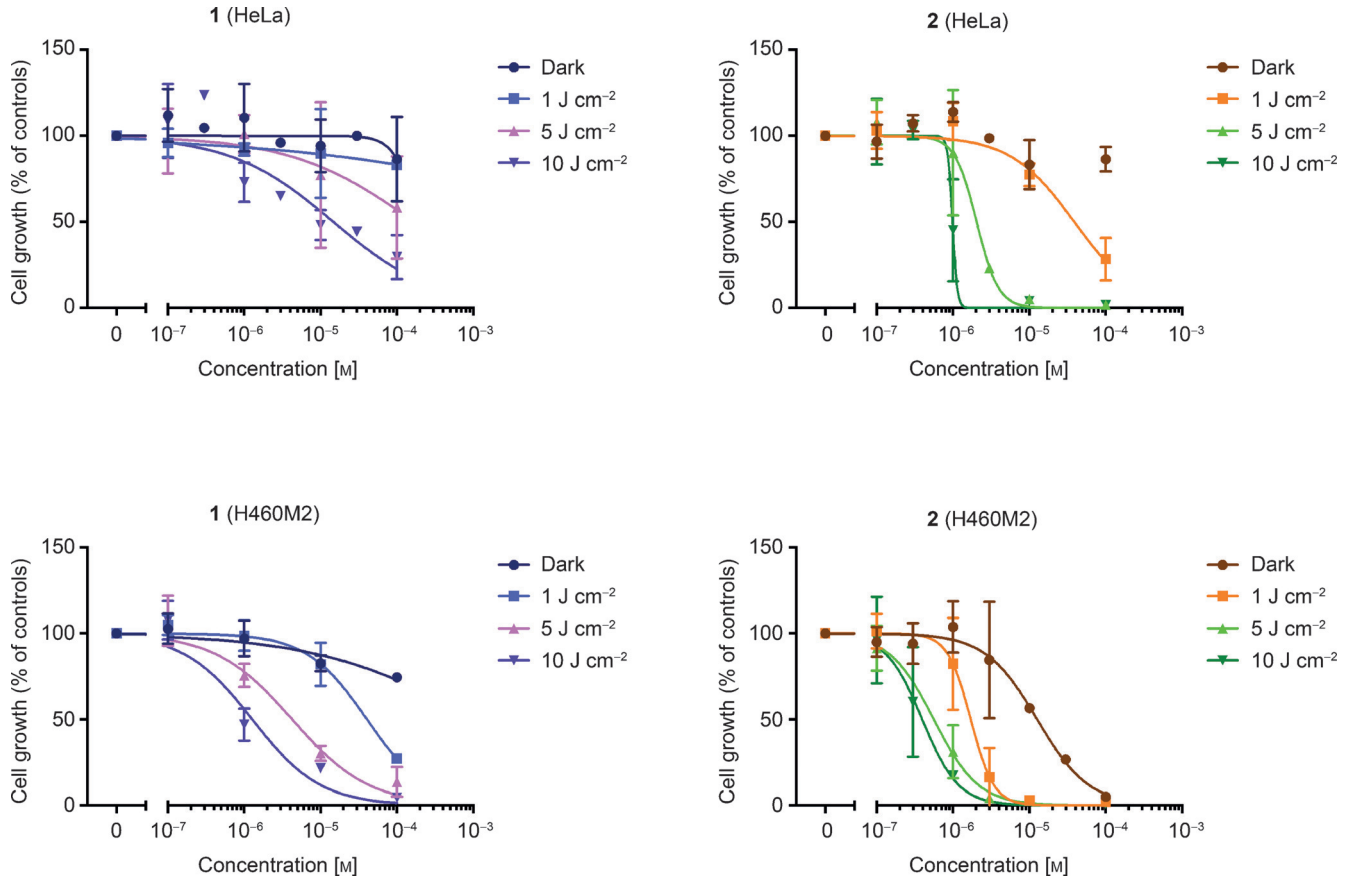

Figure 3. Light dose–effect curves for **1** and **2** as representative porphyrins. HeLa and H460M2 cells were exposed to doses from 0.1 to 100 μM for 24 h, then cells were irradiated at $\lambda = 650$ nm with a fluence rate of 14 mW cm^{-2} and total light doses ranging from 1 to 10 J cm^{-2}. Cell cytotoxicity was determined 24 h after the end of irradiation by MTT test.

a different sensitivity between dark and irradiated conditions. Of note, in compound **4**, the rhenium fragment does not enhance phototoxicity relative to **3**, suggesting that other features (hydrophilicity, permanent positive charges, one flexible arm, etc.) play a major role in determining their phototoxic properties.

As previously outlined, the prevalent mechanism of action in PDT is type II and involves the generation of $^1O_2$ after photoexcitation of the PS. For this reason, the $^1O_2$ quantum yield (Φ_Δ) was evaluated for compounds **1**–**4** in DMSO. Usually, a clinically useful PS has Φ_Δ value of ~0.5.[55] Among the investigated porphyrins, the best singlet oxygen generator is **1** ($\Phi_\Delta = 0.63$), while compounds **2**–**4** have much lower singlet oxygen quantum yields ($\Phi_\Delta = 0.31$, 0.20, and 0.19 for **2**, **3**, and **4**, respectively). However, despite being the best $^1O_2$ generator, **1** shows lower potency than **2** in the phototoxicity assay, probably due to its low cellular uptake (see below). Instead, the low Φ_Δ value of **3** and **4** might be related to their low activity on all cell lines after light irradiation. It is important to note that Φ_Δ values were determined in DMSO solutions and that a totally different environment surrounds the compound under in vitro conditions, so that other parameters—and in particular their cellular uptake—might be more important for the activity of the compounds. In other words, the phototoxic potencies of porphyrins **1**–**4** are not precisely predictable only on the basis of their Φ_Δ values. Beside being the best $^1O_2$ generator, unconjugated porphyrin **1** presents other advantageous features. It is not cytotoxic in the dark toward all three cell lines investigated, and after irradiation, its IC_{50} values on H460M2 cells decrease by two orders of magnitude.

Cellular localization studies

The cellular localization of porphyrins **1** and **3** as well as their Re^I conjugates **2** and **4** was investigated by confocal fluorescence microscopy in HeLa cells. The results are shown in Figure 4. After incubation for 2 h at a moderate concentration of 20 μM, only compound **2** displayed pronounced cellular internalization. These data are in agreement with the antiproliferative experiments. However, upon light irradiation compounds **1** and **4** showed toxicity, indicative of probable uptake. Consequently, to investigate their localization we increased the treatment concentration to 100 μM. Porphyrin **1** displayed the lowest accumulation signal inside the cell, with red luminescent speckles localized in the cytoplasm (Figure 4a). Compounds **2**–**4** showed a similar pattern with a diffused and more intense luminescence localized in the cytoplasm and to a very minor extent in the nucleoli (Figure 4, white arrows), as indicated by comparison with the 4′-6-diamino-2-phenyindole (DAPI) staining (Figure 4b,c,d). The intense red luminescence

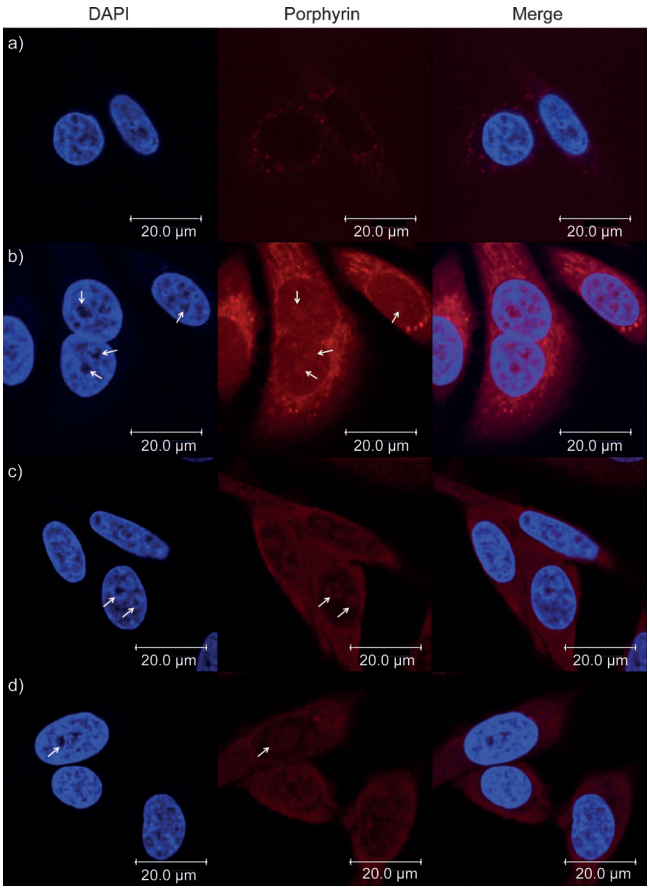

Figure 4. Fluorescence confocal microscopy images showing the pattern of HeLa cells incubated for 2 h with a) 100 μM **1**, b) 20 μM **2**, c) 100 μM **3**, and d) 100 μM **4**, fixed in formaldehyde and stained with mounting solution containing DAPI (Vectashield, 1.5 μg mL^{-1}). White arrows indicate the nucleoli.

of **2** (incubated at a concentration of 20 μM against 100 μM for **1**, **3**, and **4**) suggests that this conjugate is more efficiently taken up inside the cell than the other three compounds used in this study.

It is worth outlining that the nuclear localization of the Re conjugates, although very low, is extremely interesting in view of the Re/Tc matched pair paradigm. In fact, among radioactive sources, ^{99m}Tc emits four low-energy auger electrons per decay. Auger electron emission is a high linear energy transfer (LET) process that creates high ionization density and can cause extensive DNA fragmentation that is difficult to repair,[56] leading to cell death.[57] Auger electrons have the advantage of an extremely short effective range, which helps minimize tissue damage if delivered directly to the nuclei of cancerous cells. Thus, a ^{99m}Tc compound that localizes in the nucleus, besides being used as an imaging agent, might be itself a therapeutic agent in targeted radiotherapy for treating multiple common oncologic situations. Santos et al. showed that a Re tricarbonyl complex containing a pyrazolyldiamine chelator-bearing acridine derivative and its "hot" analogue ^{99m}Tc are internalized significantly and are retained in the nuclei of B16F1 murine melanoma cells.[58] So far, only a few reports have been published that deal with the cellular localization of rhenium tricarbonyl complexes in tumor cells,[59] showing that a variety of complexes are internalized and accumulate in cytoplasmic organelles, but only a small number reaches the nucleus. Even if localization might be explained in terms of simple chemical processes such as ionic, hydrophobic, and electrostatic hydrogen bonding interactions, in some cases, it is difficult to rationalize the experimental results on these bases.[59c]

DNA binding studies

The ability of compounds **1**–**4** to recognize and bind to DNA structures (quadruplex-forming sequences: Myc22 and H-telo; and a duplex: ds-26) was investigated using emission spectroscopy (Figures S15 and S16, Supporting Information). In all cases, interaction with DNA causes red shifting of the excitation/absorption bands of each of the four porphyrins ($\Delta\lambda \approx$ 20 nm), while different changes were observed in the emission spectra: no shift for **1**, a blue shift for **2**, and red shifts for **3** and **4**. The latter may be indicative of π–π stacking interactions. Besides these spectroscopic shifts, the compounds also display changes in emission intensity upon addition of different DNA sequences (see Figure 5).

In the case of **2**, **3**, and **4**, enhancement in the emission is more pronounced for quadruplex DNA than ds26. In contrast, compound **1** does not display selectivity for the quadruplex sequences under study versus ds26. We also carried out studies using calf thymus (ct)-DNA. As can be seen from Figure 5, the four compounds show greater enhancement of emission in the presence of quadruplexes than with ct-DNA.

The effect of the compounds on thermal stability of Myc22 DNA was investigated further by using variable-temperature circular dichroism (CD). The experiments were carried out for Myc22 (5 μM) alone and in the presence of two equivalents of each compound (Figure 6). Of the four studied compounds, **3** and **4** were found to have the greatest stabilization effect on Myc22 ($\Delta T_m = 19$ and 20 °C for **3** and **4**, respectively). Lower ΔT_m was observed for **1** (6 °C) and, surprisingly, **2** showed no

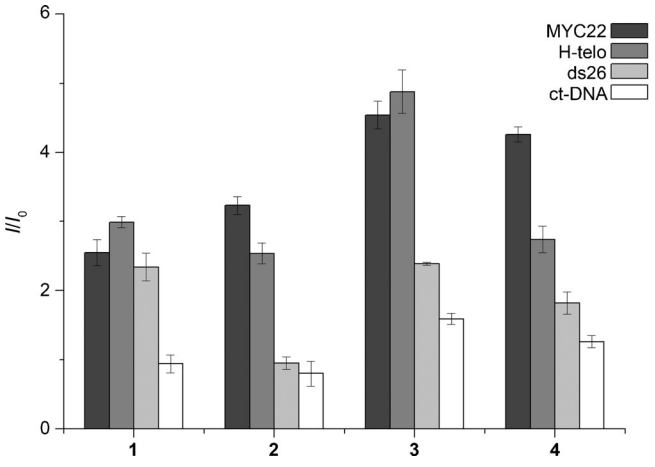

Figure 5. Bar chart showing changes in the emission intensity (determined by integration of the emission between $\lambda = 600$–850 nm) of the compounds (Tris/KCl buffer) upon addition of 20 equiv Myc22, H-telo, ds-26, and ct-DNA; λ_{ex}: **1**, 430 nm; **2**, 430 nm; **3**, 445 nm; **4**, 445 nm.

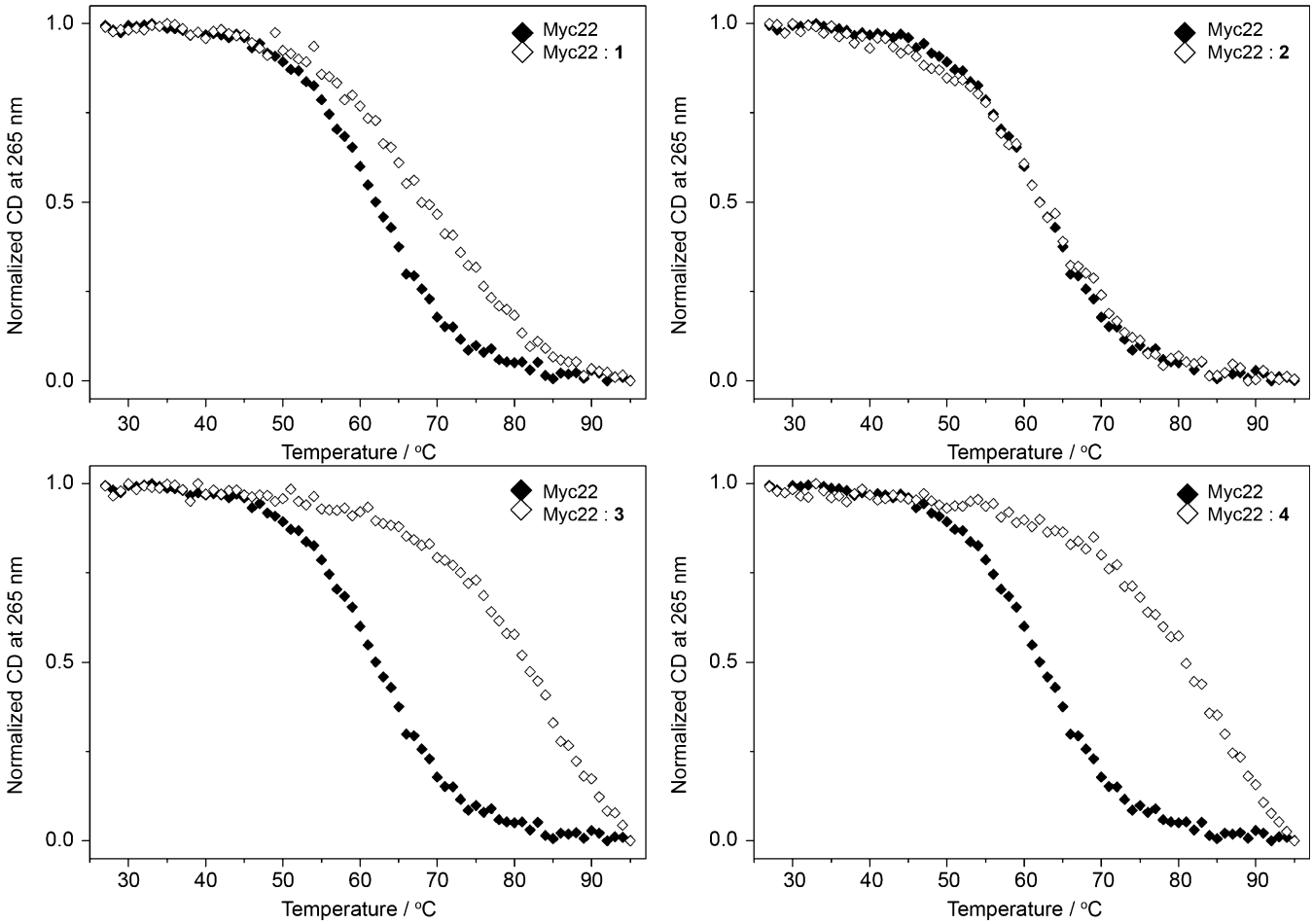

Figure 6. CD thermal denaturation profiles of Myc22 (5 μM) alone and in the presence of 2 equiv **1**, **2**, **3**, and **4**. All measurements were carried out in lithium cacodylate buffer (10 mM Li cacodylate, 99 mM LiCl, 1 mM KCl, pH 7.4); each experiment was performed in triplicate.

stabilization of Myc22 under the experimental conditions used in this experiment. The apparent lack of DNA stabilization by this compound could be due to its lower solubility in aqueous media and possibly partial precipitation of this compound during the experiment (although this was not observed by visual inspection).

DNA photocleavage

Taking into account their favorable uptake into the nucleus, their interactions with different topologies of DNA, and their phototoxic activity, we decided to investigate the effect of **1**–**4** on plasmid DNA upon light irradiation. In these experiments, circular plasmid DNA was treated with the target porphyrins and then irradiated. If the compounds induce DNA damage, a decrease in intensity of the supercoiled (intact form) band and the formation of single-strand breaks (nicked form) or double-strand breaks (linear form) bands, which migrate slower in the gel, would be observed. Supercoiled pUC18 plasmid was treated with increasing concentrations of the porphyrins (0.5–10 μM) and incubated at room temperature for 20 min. Then, taking advantage of the pronounced Soret band of **1**–**4**, we irradiated the samples at 420 nm for 22 min to achieve the same light dose used in the phototoxicity experiments (10 J cm^{-2}). A negative control of the plasmid treated with **1**–**4** (10 μM) in the dark was used for comparative purposes. As shown in Figure 7, the complexes are all able to photocleave plasmid DNA in a concentration-dependent manner. Notably, **1** and **2** demonstrated a mild effect just at 10 μM with attenuation of the supercoiled band and an increase in intensity of the nicked band. Of utmost interest, **3** and **4** showed a marked photocleavage effect already at 0.5 μM. This is most likely due to the intercalative potential of the porphyrin core and the presence of three positive charges, which are thought to maximize the DNA–complex interaction. DNA treated in the dark with the compounds (dark sample) did not show any significant alterations of the supercoiled form. Notably, complex **2** showed a shift of the supercoiled and nicked bands. This effect could be related to the intercalation of the porphyrin with the plasmid DNA.

Conclusions

Herein we report the preparation, in reasonable overall yields, of two novel versatile porphyrins, namely the tetrafunctionalized compound **1** and the monofunctionalized **3** using multi-

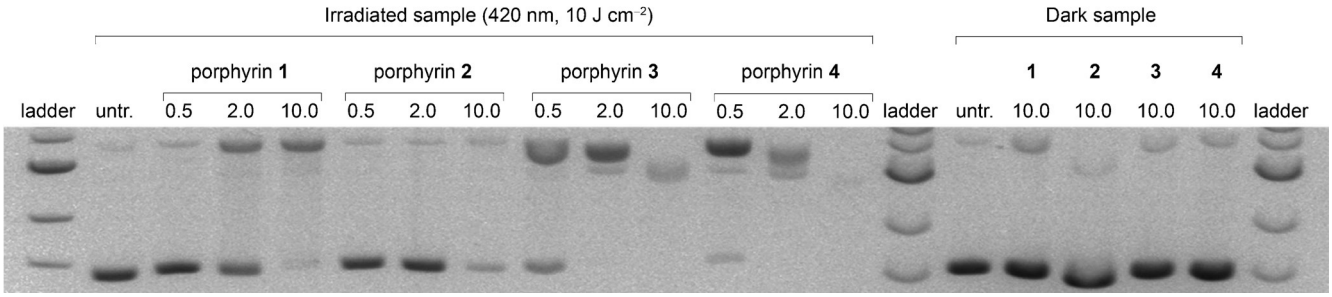

Figure 7. DNA photocleavage experiments of pUC18 plasmid treated with **1**–**4**, in the dark and upon light irradiation at $\lambda = 420$ nm for 22 min (10 J cm^{-2}); untr. = DNA untreated; concentrations are expressed in μM.

step syntheses. These porphyrins bear either four (**1**) or one (**3**) chelating TACN fragments at the *meso* positions connected through flexible and hydrophilic linkers. We demonstrated that both porphyrins **1** and **3** can bind the *fac*-{Re(CO)$_3$}$^+$ fragment to give the tetracationic conjugates **2** and **4**, respectively, in good yields. The presence of one or four hydrophilic spacers containing the ethylenedioxy groups, as well as the positive charges on the complexes contribute to the water solubility of the unconjugated porphyrins as well as of their corresponding Re derivatives. Because the Re(CO)$_3$ fragment is rather hydrophobic, conjugate **2** is only slightly soluble in water, even if it bears four positive charges.

All compounds were investigated for in vitro cell growth inhibition toward cervical cancer (HeLa), lung cancer (H460M2), and non-tumorigenic (HBL-100) cell lines. Importantly, all compounds are nontoxic up to a concentration of 100 μM in the dark on the cell lines studied in this work, except for the Re conjugate **2**, which has IC_{50} values of ~7 and 34 μM on H460M2 and HBL-100 cells, respectively. Upon light irradiation at $\lambda = 650$ nm, compounds **1** and **2** showed much better phototoxic properties than the monofunctionalized **3** and **4**. In particular, Re–porphyrin conjugate **2** showed remarkable phototoxicity on HeLa cells, similar to hypericin and photofrin. The phototoxic activity of **2** and its lack of dark toxicity on HeLa cells suggest a selective use of this compound in all tumor cell lines that show a selective sensitivity between the dark and irradiation experiments. The unconjugated parent porphyrin **1** had excellent phototoxic activity on H460M2 cells, with a PI > 77 at a light dose of 10 J cm^{-2}. Notably, the light dose used during the course of our experiments is similar to, or even lower than, that used for related compounds. This clearly guarantees the absence of damage to untreated cells.

The intracellular localization studies in HeLa cells outlined a minimal cellular penetration for **1** that might be related to its low photoactivity on this cell line. Instead, the Re conjugate **2** showed very good cellular uptake. This might explain its better photoactivity on the same cell line, although **2** is less efficient at producing $^1O_2$ than **1**. Compounds **3** and **4** were found to be more efficient than **1** and **2** at binding DNA (with some selectivity for quadruplex versus duplex) as well as in DNA photocleavage.

Upon Re coordination, we observed an enhancement in the phototoxic activity of the tetrafunctionalized porphyrin **1**, whereas the presence of the metal center did not substantially affect the photoactivity of the monofunctionalized porphyrin **3** on all the cell lines studied in this work. These overall results do not clearly indicate the role of the metal center in influencing the phototoxic properties of porphyrins, but at the same time suggest that it does not represent a negative factor. Therefore, the possibility of obtaining the corresponding ^{99m}Tc conjugates is a very interesting perspective to develop new therapeutic agents. We are currently assessing this opportunity, and our results will be published in due course.

Experimental Section

Synthesis and characterization

One- and two-dimensional (H–H COSY and HSQC) NMR spectra were recorded on a Varian 500 spectrometer (500 MHz for ^{1}H, 470 MHz for ^{19}F). All spectra were run at room temperature. ^{1}H NMR chemical shifts were referenced to the peak of residual non-deuterated solvent ($\delta = 7.26$ for $CDCl_3$, 3.31 for CD_3OD, 4.34 for CD_3CN, 2.50 for [D_6]DMSO). ^{19}F NMR shifts are referenced to $CFCl_3$ as internal standard. UV/Vis spectra were obtained at $T = 25\,^\circ$C on a Jasco V-500 UV/Vis spectrophotometer equipped with a Peltier temperature controller, using 1.0 cm path-length quartz cuvettes (3.0 mL). IR spectra were recorded on a PerkinElmer Spectrum RXI FTIR spectrophotometer. Mass spectra were obtained by positive and negative ESI-MS using a Bruker Esquire ESI-MS instrument. ESI HRMS were obtained using a Bruker maXis instrument.

Column chromatography was performed on silica gel 60 Å (Merck, 230–400 mesh ASTM), eluting with chloroform/ethanol mixtures as specified below. The reactions were monitored by TLC (silica gel/UV 254, 0.25 mm, glass or aluminum support).

Porphyrin intermediates **6** and **8** and Re^I precursor *fac*-[Re(CO)$_3$(dmso-O)$_3$](CF$_3$SO$_3$)[60] were prepared according to published procedures.[27,30,61] All chemicals were purchased from Sigma–Aldrich and were used without further purification unless otherwise specified.

The porphyrins and their Re conjugates precipitate with variable amounts of crystallization solvent, depending on the batch. For this reason elemental analysis of such conjugates did not afford reliable and reproducible results, and the values are not reported here (typically, some of the elemental analysis values, especially for C, differ from calculated values by > 0.5 %). Nevertheless, the purity calculated from elemental analysis data was always > 95 %, and the proposed formulae are all consistent with NMR, ESI MS and ESI

HRMS spectra. Of note, the ^{13}C NMR spectra are not reported, as the solubility of compounds **1–4** in CD_3OD at the maximum extent was insufficient to observe all the carbon resonances, especially of the quaternary carbons, even after an accumulation time of 72 h.

Di-*tert*-butyl-[1,4,7]-triazacyclononane-1,4-dicarboxylate (diBoc-TACN) (10): To a solution of TACN (500.5 mg, 3.87 mmol) in $CHCl_3$ (10 mL), TEA (744 μL, 5.34 mmol) was added. To this transparent solution a solution of $(Boc)_2O$ (1.53 g, 7.00 mmol) in $CHCl_3$ (20 mL) was added dropwise under an argon atmosphere in 4 h at room temperature. The reaction mixture was stirred overnight under an argon atmosphere at room temperature. The reaction was monitored by TLC (EtOAc/EtOH 10:1, $R_f = 0.3$). The solvent was removed under reduced pressure to give the product as a white oil. The product was dissolved in EtOAc (100 mL) and then washed with 4% $NaHCO_3$ (100 mL) and brine (100 mL×2). The organic phase was washed with 10% aqueous citric acid (100 mL×3) and the product moved in the water phase. NaOH 10% was added under ice-cooling until the water phase was adjusted to pH 10 and the product was extracted with CH_2Cl_2 (100 mL×3). The organic solution was dried over Na_2SO_4 and the solvent was removed under reduced pressure to give the product as a white oil. Yield: 718 mg (56%); ^1H NMR ($CDCl_3$): $\delta = 3.49$ (m, 2H, CH_2 c), 3.43 (m, 2H, CH_2 c), 3.31 (m, 2H, CH_2 b), 3.25 (m, 2H, CH_2 b), 2.94 (m, 4H, CH_2 a), 1.48 ppm (s, 18H, CH_3 Boc); ESI-MS *m/z* 330.2 $[M+H]^+$, 325.2 $[M+Na]^+$.

1,4-Bis(*tert*-butyloxycarbonyl)-1,4,7-triazacyclononane-7-benzylacetate (diBocTACNCbz) (11): To a solution of **10** (718 mg, 2.18 mmol) and TEA (608 μL, 4.36 mmol) in $CHCl_3$ (12 mL) a solution of benzyl bromoacetate (1.26 g, 5.50 mmol) in $CHCl_3$ (23 mL) was added dropwise under ice-cooling in 1 h. The solution was stirred for 48 h at room temperature and the reaction was monitored by TLC (CH_2Cl_2/EtOH 95:5, $R_f = 0.6$). The solvent was removed under reduced pressure to give a yellow oil that was purified by column chromatography (CH_2Cl_2/EtOH, 97:3, then 95:5) to afford the pure product as a yellow oil. Yield: 926 mg (89%); ^1H NMR ($CDCl_3$): $\delta =$ 7.35 (m, 5H, H Ph), 5.13 (t, 2H, CH_2 e), 3.49 (s, 2H, CH_2 d), 3.45 (m, 4H, CH_2 c), 3.26 (m, 2H, CH_2 b), 3.20 (m, 2H, CH_2 b), 2.84 (m, 4H, CH_2 a), 1.46 (s, 9H, CH_3 Boc), 1.45 ppm (s, 9H, CH_3 Boc); ESI-MS *m/z* 478.3 $[M+H]^+$, 500.3 $[M+Na]^+$, 516.3 $[M+K]^+$.

1,4-Bis(*tert*-butyloxycarbonyl)-1,4,7-triazacyclononane-7-acetic acid (2-(diBoc)TACN acetic acid) (5): To a deoxygenated solution of **11** (926 mg, 1.94 mmol) in CH_3OH (25 mL) Pd/C was slowly added, then the reaction flask was purged with H_2 several times. After 24 h the catalyst was removed by filtration over a Celite pad and the solvent was evaporated under reduced pressure to give a white crystalline solid. TLC: CH_2Cl_2/EtOH 9:1, $R_f = 0.3$; Yield: 686 mg (91%); ^1H NMR ($CDCl_3$): $\delta = 3.56–3.18$ (m, 8H, CH_2 b + CH_2 c), 3.39 (s, 2H, CH_2 d) 2.77–2.65 (m, 4H, CH_2 a) 1.48 (s, 9H, CH_3 Boc), 1.49 ppm (s, 9H, CH_3 Boc); ESI-MS *m/z* (negative mode) 386.1 $[M-H]^-$, (positive mode): 388.2 $[M+H]^+$, 410.2 $[M+Na]^+$.

Boc-protected porphyrin 7: To a solution of **5** (54.44 mg, 0.14 mmol) in anhydrous DMF (3 mL), HOBt (28.51 mg, 0.21 mmol) and *N*-(3-dimethylaminopropyl)-*N'*-ethylcarbodiimide hydrochloride (EDCI) (40.6 mg, 0.21 mmol) were added. The solution was stirred for 30 min, then a purple solution of the porphyrin **6** (0.0234 mmol) and DMAP (28.80 mg, 0.23 mmol) in anhydrous DMF (4 mL) was added. The reaction was monitored by TLC (CH_2Cl_2/EtOH 9:1, $R_f = 0.3$). The reaction solution was stirred overnight at room temperature shielded from light. The product was purified by column chromatography (CH_2Cl_2/EtOH 90:10, then 85:15) to obtain 43.2 mg of a purple solid (66% yield); ^1H NMR ($CDCl_3$): $\delta = 8.83$ (s, 8H, βH), 8.27 (dd, 16 H *m*Ph + *o*Ph), 7.74 (m, 2H, NHCO), 7.66 (m, 2H, NHCO), 7.38 (m, 4H, NHCO), 3.83 (m, 8H, CH_2NH + 8H, CH_2O), 3.72 (m, 16H, CH_2O), 3.62 (m, 8H, CH_2O), 3.50 (m, 16H, CH_2 c + CH_2NH), 3.35 (m, 16H, CH_2 b), 3.21 (m, 8H, CH_2 d), 2.67 (m, 16H, CH_2 a), 1.48, 1,46, 1.42 (s, 72H, CH_3 Boc), −2,78 ppm (br s, 2H, NH); UV/Vis (CH_2Cl_2): λ_{max} (relative intensity %) = 419.5 (100), 515.2 (4.3), 550.2 (2.1), 590.2 (1.5), 645.9 nm (1.1).

Porphyrin 1: Porphyrin **7** (14.54 mg, 0.0052 mmol) was dissolved in CH_2Cl_2 (1.5 mL) to obtain a purple solution. To this solution TFA (1.5 mL) was added and the solution turned deep green. The solution was stirred for 4 h shielded from light, and then the solvent was removed under reduced pressure until the elimination of TFA was complete, to give a green–blue product. The porphyrin as TFA salt (0.0052 mmol) was dissolved in the minimum amount of CH_3OH to obtain a deep green solution. To this solution 30 μL (0.20 mmol) of TEA were added and the solution turned purple, that indicated the pH changed to basic. The product was precipitated by adding Et_2O dropwise to the solution. The solid was extensively washed with Et_2O and dried under vacuum. (10 mg, yield 97%); ^1H NMR (CD_3OD): $\delta = 8.88$ (br s, 8H, βH), 8.34 (d, 8H, H Ph, $J = 8.2$ Hz), 8.30 (d, 8H, H Ph, $J = 8.2$ Hz), 3.83 (m, 8H, CH_2O), 3.78 (m, 16H, $CH_2O + CH_2NH$), 3.73 (m, 8H, CH_2O), 3.64 (m, 8H, CH_2O), 3.47 (m, 16H, CH_2 d + CH_2NH), 3.22 (m, 16H, CH_2 c), 3.04 (m, 16H, CH_2 b), 2.86 ppm (m, 16H, CH_2 a); UV/Vis (CH_3OH): λ_{max} ($\varepsilon \times 10^{-3}$) = 416 (250), 513 (11), 547 (4.9), 590 (2.8) 645 nm (2.4 $dm^3 mol^{-1} cm^{-1}$); ESI-MS *m/z* 1989.9 $[M+H]^+$; ESI HRMS calcd for $[C_{104}H_{146}N_{24}O_{16}]/z$ $[M+3H]^{3+}$ 663.37829, found 663.71765, calcd for $[M+4H]^{4+}$ 497.78372 found 498.04085, calcd for $[M+5H]^{5+}$ 398.42697 found 398.63419.

Porphyrin–Re^I conjugate 2: Porphyrin **1** (25.08 mg, 0.0126 mmol) was dissolved in anhydrous CH_3OH (20 mL). To this solution *fac*-$[Re(CO)_3(dmso\text{-}O)_3](CF_3SO_3)$ (49.91 mg, 0.0764 mmol, 6 equiv) was added. The stirred mixture was held at reflux under argon and was shielded from light for 48 h. The reaction was monitored by ^1H NMR spectroscopy after 6, 13, and 30 h and by TLC (CH_3CN/H_2O/KNO_3 $R_f = 0.46$). After the solvent was removed under reduced pressure, the solid was dissolved in the minimum amount of CH_3OH and precipitated by adding Et_2O dropwise. The product was then extensively washed with Et_2O and CH_2Cl_2 to give a brown product (30.1 mg, yield 65%); ^1H NMR (CD_3OD): $\delta = 8.32$ (dd, 16H, *o*Ph + *m*Ph), 8.89 (br s, 8H, βH), 6.83 (s, 8H, NH TACN), 4.16 (s, 8H, CH_2 d), 3.83 (m, 8H, CH_2O), 3.78 (m, 16H, $CH_2O + CH_2NHCO$), 3.72 (m, 8H, CH_2O), 3.63 (t, 8H, CH_2O, $J = 5.5$ Hz), 3.44 (t, 8H, CH_2NHCO, $J = 5.5$ Hz), 3.23 (m, 16H, CH_2 a + CH_2 TACN), 3.13 (m, 8H, CH_2 a), 2.90 (m, 8H, CH_2 TACN), 2.70 (m, 8H, CH_2 TACN), 2.59 (m, 8H, CH_2 TACN); UV/Vis (CH_3OH): λ_{max} ($\varepsilon \times 10^{-3}$) = 416 (217), 516 (10), 554 (5.0), 596 (3.1), 649 nm (2.3 $dm^3 mol^{-1} cm^{-1}$); ESI HRMS calcd for $[C_{120}H_{170}N_{24}O_{28}Re_4]/z$ $[M]^{4+}$ 785.77116, found 785.77425; IR (KBr): $\tilde{\nu} = 2028$ (CO), 1910 cm^{-1} (CO).

Boc-protected porphyrin 9: To a solution of **5** (14.34 mg, 0.0370 mmol, 1.44 equiv) in anhydrous DMF (1.5 mL) HOBt (7.52 mg, 0.0556 mmol, 2.17 equiv) and EDCI (10.64 mg, 0.0555 mmol, 2.17 equiv) were added and the resulting solution was stirred for 30 min. To this solution a purple solution of the porphyrin **8** (30.07 mg, 0.0256 mmol) and DMAP (7.65 mg, 0.0626 mmol, 2.44 equiv) in anhydrous DMF (1.5 mL) was added. The coupling was performed in a microwave oven reactor (ramp time: 10 s, hold time: 6 min, $T = 60\,^\circ C$, $P = 1720$ kPa, power: 30 W). The reaction was monitored by TLC (CH_3CN/KNO_3/H_2O 4:0.3:1, $R_f =$ 0.38). The charged porphyrin **9** was purified by repeated precipitation (CH_3OH/Et_2O and CH_3CN/Et_2O) and extensive washing with Et_2O and CH_2Cl_2 to remove the excess either of reagents and of

the ligand. Yield: 65% (26.27 mg); ^{1}H NMR (CD_3CN): $\delta = 9.12$ (m, 6H, 2,6py), 9.07 (m, 6H, βH), 8.95 (m, 2H, βH), 8.82 (m, 6H, 3,5py), 8.30 (dd, 4H, *o*Ph + *m*Ph), 4.70 (s, 3H, CH_3py), 4.69 (s, 6H, CH_3py), 3.75 (m, 2H, CH_2O), 3.70 (m, 4H, $CH_2O + CH_2NH$), 3.65 (m, 2H, CH_2O), 3.55 (t, 2H, CH_2O, $J = 5.6$ Hz), 3.37 (m, 6H, $CH_2NH + CH_2$ c), 3.23 (m, 4H, CH_2 b), 3.09 (m, 2H, CH_2 d), 2.59 (m, 4H, CH_2 a), 1.43, 1.42, 1.36 (s, 18H, CH_3Boc), $^-$2.96 ppm (s, 2H, NH pyrrole); UV/Vis (CH_3OH): λ_{max} (relative intensity %) = 422 (100), 516 (8.3), 553 (3.9), 589 (3.3), 648 nm (1.3); ESI-MS *m/z* 1205.7 $[M]^+$, 603.1 $[M]^{2+}$.

Porphyrin 3: To a solution of porphyrin **9** (26.27 mg, 0.0166 mmol) in CH_3OH (2 mL) TFA (800 μL) was added. The solution was stirred for 3 h shielded from light, and then the solvent was removed under reduced pressure until the complete elimination of TFA, to give the product as TFA salt. The deep green–brown solid was dissolved in 1 mL CH_3OH. To this solution 10 μL TEA were added. The product was precipitated by adding Et_2O dropwise to the solution and was then extensively washed with Et_2O. The product was obtained as a purple solid (21.83 mg, yield 98%); ^{1}H NMR (CD_3CN): $\delta = 9.13$ (d, 6H, 2,6py, $J = 6.4$ Hz), 9.06 (m, 6H, βH), 8.98 (m, 2H, βH), 8.83 (d, 6H, 3,5py, $J = 6.5$ Hz), 8.30 (dd, 4H, *o*Ph + *m*Ph), 7.83 (t, NHCO, 1H, $J = 5.4$ Hz), 4.69 (s, 3H, CH_3py), 4.70 (s, 6H, CH_3py), 3.79 (t, 2H, CH_2O, $J = 5.4$ Hz), 3.72 (m, 4H, $CH_2O + CH_2NH$), 3.66 (m, 2H, CH_2O), 3.58 (t, 2H, CH_2 2, $J = 5.5$ Hz), 3.37 (s, 2H, CH_2 d), 3.38 (m, 2H, CH_2NH), 3.29 (m, 4H, CH_2 b), 3.02 (m, 4H, CH_2 c), 2.82 ppm (t, 4H, CH_2 a, $J = 5.4$ Hz); TLC: $R_f = 0.06$ $CH_3CN/KNO_{3\ sat}/H_2O$ 4:0.3:1; UV/Vis (CH_3CN): λ_{max} ($\varepsilon \times 10^{-3}$) = 423 (157), 517 (15), 553 (8.3), 590 (6.4), 646 nm (3.2 $dm^3 mol^{-1} cm^{-1}$); ^{19}F NMR (CD_3CN): $\delta = -75.62$ ppm (CF_3COO^-); ESI-MS *m/z* 1005.6 $[M]^+$, 502.8 $[M]^{2+}$; ESI HRMS calcd for $[C_{59}H_{65}N_{12}O_4]/z$ $[M]^{3+}$ 335.17451, found 335.17451.

Porphyrin–Re^I conjugate 4: Porphyrin **3** (14.32 mg, 0.0106 mmol) was dissolved in anhydrous CH_3OH (5 mL). To this solution *fac*-[Re(-CO)$_3$(dmso-O)$_3$](CF_3SO_3) (10.27 mg, 0.0157 mmol, 1.5 equiv) was added. The reaction was performed in a microwave oven reactor (first step: $T = 65$ °C, ramp time: 10 min, hold time: 30 s, $P =$ 1720 kPa, power: 25 W; second step: $T = 110$ °C, ramp time: 10 min, hold time: 10 min, $P = 1720$ kPa, power: 30 W). The reaction was monitored by TLC ($CH_3CN/KNO_3/H_2O$, 4:0.3:1, $R_f = 0.32$). The solvent was then removed under reduced pressure. The product was dissolved in the minimum amount of CH_3OH and precipitated with Et_2O, then it was washed with Et_2O and CH_2Cl_2 to remove excess complex to obtain 13.76 mg of the pure product (yield 73%); ^{1}H NMR (CD_3CN): $\delta = 9.12$ (d, 6H, 2,6py, $J = 6.2$ Hz), 9.06 (m, 6H, βH), 8.98 (m, 2H, βH), 8.83 (d, 6H, 3,5py, $J = 6.5$ Hz), 8.31 (dd, 4H, *o*Ph + *m*Ph), 7.66 (t, NHCO, 1H, $J = 6.2$ Hz), 7.12 (t, NHCO, 1H, $J =$ 7.5 Hz), 5.90 (m, 2H, NH TACN), 4.96 (m, 9H, CH_3py), 4.12 (s, 2H, CH_2 d), 3.78 (t, 2H, CH_2O, $J = 5.5$ Hz), 3.72 (m, 4H, $CH_2O + CH_2$ 8), 3.66 (m, 2H, CH_2O), 3.57 (t, 2H, CH_2 2$J = 5.5$ Hz), 3.38 (m, 2H, CH_2 1), 3.31 (m, 2H, CH_2 c), 3.21 (m, 4H, CH_2 a), 3.00 (m, 2H, CH_2 b), 2.72 (m, 2H, CH_2 c), 2.63 ppm (m, 2H,CH_2 b); UV/Vis (CH_3CN): λ_{max} ($\varepsilon \times 10^{-3}$) = 424 (222), 517 (15), 553 (6.0), 590 (4.5), 646 nm (0.7 $dm^3 mol^{-1} cm^{-1}$); ^{19}F NMR (CD_3CN): $\delta = -75.30$ (CF_3COO^-), -79.28 ppm ($CF_3SO_3^-$); ESI HRMS calcd for $[C_{63}H_{71}N_{12}O_7Re]/z$ $[M]^{4+}$ 323.62774, found 323.62772; IR (KBr): $\tilde{\nu} = 1977$ (CO), 2104 cm^{-1} (CO).

Biological methods

Cell culture: Human cervical carcinoma cells (HeLa) were cultured in DMEM (Euroclone) supplemented with 5% fetal bovine serum (FBS, Gibco), 100 UI mL^{-1} penicillin, 100 μg mL^{-1} streptomycin, 2 mM L-glutamine. The non-small-cell lung carcinoma cell line (H460M2) was grown in RPMI (Euroclone) supplemented with 5% FBS (Gibco), HEPES (Euroclone), 100 UI mL^{-1} penicillin, 100 μg mL^{-1} streptomycin, 2 mM L-glutamine. HBL-100 non-tumorigenic epithelial cells were grown in McCoy's (Sigma) supplemented with 10% FBS (Gibco), 100 UI mL^{-1} penicillin, 100 μg mL^{-1} streptomycin, 2 mM L-glutamine. The cells were cultured at 37 °C and in 5% CO_2 humidified atmosphere.

Cell phototoxicity: Cells were sown at 10000 per well on 96-well plates and allowed to grow 24 h. Then they were incubated for 24 h with 0.1–100 μM solutions of each compound, obtained by serial dilutions of stock solutions (freshly prepared in DMSO at a concentration of 10^{-2} M) with complete medium. Maximum DMSO concentration in the cell incubation medium was ≤0.3% *v/v*. Thereafter, the media containing compounds were replaced with drug-free medium and cells were irradiated at $\lambda = 650$ nm at a fluence rate of 14 mW cm^{-2} for a time such that the total light dose was either 1, 5, or 10 J cm^{-2} (71 s; 5 min, 57 s; or 11 min, 54 s). The illumination was performed with a LED board equipped with dedicated software. The LED board and software were assembled and set up by F. Armani and G. Verona (A.P.L. Laboratory of the Department of Engineering and Architecture at the University of Trieste). The LED board is equipped with 96 red LEDs (L-53SRC-E, Kingbright) arranged in order to fit with the 96 wells of the cell culture plates. The emitted power (mW) at the end of the optical fiber was measured with an Ophir NOVA Laser Measurement power meter. Control experiments performed in the absence of any photosensitizer indicated that light doses up to 10 J cm^{-2} cause no evident cell damage. A plate similarly treated, but not exposed to light was used as reference for dark cytotoxicity under the same experimental conditions. Analysis of cell phototoxicity by MTT assay was performed after further 24 h of incubation and compared with the values of control cells without light irradiation. Briefly, MTT dissolved in phosphate-buffered saline (PBS, 5 mg mL^{-1}) was added (10 μL per 100 μL medium) to all wells, and the plates were then incubated at 37 °C with 5% CO_2 and 100% relative humidity for 4 h. After this time, the medium was discarded, and 200 μL DMSO were added to each well according to the method of Alley et al.[62] Absorbance units were measured at $\lambda = 570$ nm on a SpectraCount Packard instrument (Meriden, CT, USA). IC_{50} values were calculated from dose–effect curves and are the mean ± SD of at least three separate experiments. The fitting procedure applied is a nonlinear regression performed with GraphPad Prism version 6 for Mac OS X version 6.0b (GraphPad Software, San Diego, CA, USA). Experiments were conducted in quadruplicate and repeated thrice.

Statistical analysis: Data obtained in the experiments were subjected to statistical analysis of variance (ANOVA) and Tukey–Kramer post-test, or to unpaired *t* test performed using GraphPad InStat version 3.06 for Windows (GraphPad Software, San Diego, CA, USA).

Singlet oxygen production: The quantum yield (Φ_Δ) of singlet oxygen generated by compounds **1**–**4** upon photoexcitation was measured using 9,10-dimethylanthracene (DMA) as substrate. Typically, 3 mL of 0.133 mM $CHCl_3$ solution of DMA and 0.4 μL solution of the porphyrin (0.4 A at Soret band maximum, ≈10 mM) in DMSO were placed in a luminescence quartz cuvette of 1 cm optical path and irradiated in a RPR100 Rayonet Chamber Reactor (Southern New England Ultraviolet Company) complete with two lamps of $\lambda = 420$ nm light for different periods of time. The fluence rate was 2.57 mW cm^{-2}. The first-order rate constant of the photooxidation of DMA by $^1O_2$ was obtained by plotting $A_0 - A$ as a function of the irradiation time *t*, in which A_0 and *A* represent the absorbance intensity at time 0 and at time *t*, respectively. The rate constant was then converted into $^1O_2$ quantum yield by compari-

son with the rate constant for DMA photo-oxidation sensitized by TPP, (for which Φ_Δ was shown to be 0.55) and with the absorbance correction factor $I = I_0{}^*(1-10^{-A\lambda})$, where I_0 is the light intensity of the irradiation source in the irradiation interval, and A is the absorbance of the sample at wavelength λ.

Fluorescence microscopy: Cells were grown on 18 mm Menzel glass coverslips (Menzel, Germany) at a density of 2.5×10^5 cells mL^{-1} and incubated with the indicated compound. Upon 2 h treatment, cells were fixed for 15 min at room temperature in 4% formaldehyde solution (4% formaldehyde (*w*/*v*) in 1×PBS) and mounted on microscopy slides. Fixed cells were examined with a CLSM Leica SP5 confocal microscope (DAPI $\lambda_{ex}=405$ nm, $\lambda_{em}=430$–500 nm; porphyrin $\lambda_{ex}=514$ nm, $\lambda_{em}=600$–700 nm) using 63×1.20 oil-immersion lenses.

DNA preparation: All oligonucleotides, namely Myc22 (5′-TGA GGG TGG GTA GGG TGG GTA A-3′), H-telo (5′-AGG GTT AGG GTT AGG GTT AGG G-3′), and ds-26 (5′-CAA TCG GAT CGA ATT CGA TCC GAT TG-3′) were purchased from Eurogentec and used without further purification. ct-DNA was purchased from Sigma–Aldrich and used as received. The oligonucleotides (for both emission and CD spectroscopic studies) were dissolved in Milli-Q water to yield 1 mM stock solution which was stored at −20 °C and defrosted on the day when a given experiment was carried out. The 1 mM oligonucleotide stock solution was further diluted using appropriate buffer to the desired concentration on the day of the experiment. The concentration of oligonucleotides was determined by UV/Vis spectroscopy using appropriate extinction coefficients at $\lambda=260$ nm. For the emission titrations, concentration of the compound being studied was kept constant (at 5 μM); the concentration of DNA added during the titrations (after appropriate dilutions from the stock solution) ranged between 0 and 40 μM. For the variable-temperature CD spectroscopic studies the final concentrations of DNA and compound were 5 and 10 μM, respectively.

Compound preparation for DNA binding studies: Compounds were dissolved in Milli-Q water to yield 1 mM solutions (except for **2**, which was dissolved in DMSO). These solutions were diluted with the buffer to give a final concentration of 5 μM for the emission titrations and 10 μM variable-temperature CD studies. Unless stated otherwise, all measurements were performed in Tris·HCl (50 mM) buffer containing 100 mM KCl (pH 7.4). Emission and excitation spectra were recorded on Varian Cary Eclipse Spectrometer. Circular dichroism measurements were carried out using a Jasco J-715 Spectropolarimeter.

DNA photocleavage: DNA photocleavage experiments were performed according to a method reported recently by our group.[63] More specifically, supercoiled pUC18 plasmid (0.20 μg) was incubated with **1**–**4** at increasing concentrations in buffer (50 mM Tris·HCl, 18 mM NaCl, pH 7.2) and at $\lambda=420$ nm for 22 min (10 J cm^{-2}) in a RPR100 Rayonet Chamber Reactor (Southern New England Ultraviolet Company). A series of negative controls of the plasmid treated with the highest concentrations of **1**–**4** in the dark was used for comparative purposes. After irradiation the samples were added with loading buffer (250 mg xylene cyanol in 33 mL 150 mM Tris·HCl buffer, pH 7.6) and analyzed by electrophoresis in agarose 0.8% in 1×TBE (diluted from a 10× solution of 108 g Tris·HCl, and 55 g of H_3BO_3 in 900 mL H_2O) at 70 V (BioRad Power Pack 1000) for 1.5 h. The gel was pre-stained with GelRed (1:10000, Biotium), photographed and quantified with an AlphaDigiDoc 1000 CCD camera (Buchner Biotec AG) and AlphaImager software (version 1.3.0.7.).

Acknowledgements

Financial Support from the Swiss National Science Foundation (Professorships PP00P2_133568 and PP00P2_157545 to G.G.), the Stiftung für Wissenschaftliche Forschung of the University of Zurich (G.G.), the UBS Promedica Stiftung (R.R. and G.G), the Novartis Jubilee Foundation (R.R and G.G.), the Casali Foundation (T.G.), the Beneficentia Stiftung (E.A.), the University of Zurich (G.G.), the UK's Engineering and Physical Sciences Research Council grant number EP/H005285/1 (A.L. and R.V.), and the COST Action CM1105 (G.G., R.V., A.B., and E.A.) is gratefully acknowledged. The authors thank the Center for Microscopy and Image Analysis of the University of Zurich for access to state-of-the-art equipment.

Keywords: antitumor agents · photodynamic therapy (PDT) · phototoxicity · porphyrins · rhenium

[1] P. Agostinis, K. Berg, K. A. Cengel, T. H. Foster, A. W. Girotti, S. O. Gollnick, S. M. Hahn, M. R. Hamblin, A. Juzeniene, D. Kessel, M. Korbelik, J. Moan, P. Mroz, D. Nowis, J. Piette, B. C. Wilson, J. Golab, *Ca-Cancer J. Clin.* **2011**, *61*, 250–281.
[2] D. E. J. G. J. Dolmans, D. Fukumura, R. K. Jain, *Nat. Rev. Cancer* **2003**, *3*, 380–387.
[3] M. R. Hamblin, T. Hasan, *Photochem. Photobiol. Sci.* **2004**, *3*, 436–450.
[4] T. Maisch, *Mini-Rev. Med. Chem.* **2009**, *9*, 974–983.
[5] T. J. Dougherty, C. J. Gomer, B. W. Henderson, G. Jori, D. Kessel, M. Korbelik, J. Moan, Q. Peng, *J. Natl. Cancer Inst.* **1998**, *90*, 889–905.
[6] R. Bhuvaneswari, Y. Y. Gan, K. C. Soo, M. Olivo, *Cell. Mol. Life Sci.* **2009**, *66*, 2275–2283.
[7] A. P. Castano, P. Mroz, M. R. Hamblin, *Nat. Rev. Cancer* **2006**, *6*, 535–545.
[8] N. L. Oleinick, H. H. Evans, *Radiat. Res.* **1998**, *150*, S146–S156.
[9] R. Bonnett, *Chem. Soc. Rev.* **1995**, *24*, 19–33.
[10] A. Leonidova, V. Pierroz, R. Rubbiani, Y. Lan, A. G. Schmitz, A. Kaech, R. K. O. Sigel, S. Ferrari, G. Gasser, *Chem. Sci.* **2014**, *5*, 4044–4056.
[11] J. Moan, K. Berg, *Photochem. Photobiol.* **1991**, *53*, 549–553.
[12] E. Skovsen, J. W. Snyder, J. D. Lambert, P. R. Ogilby, *J. Phys. Chem. B* **2005**, *109*, 8570–8573.
[13] J. Moan, P. Juzenas, *J. Environ. Pathol. Toxicol. Oncol.* **2006**, *25*, 29–50.
[14] A. M. R. Fisher, A. L. Murphree, C. J. Gomer, *Lasers Surg. Med.* **1995**, *17*, 2–31.
[15] G. Palumbo, *Expert Opin. Drug Delivery* **2007**, *4*, 131–148.
[16] A. Juarranz, P. Jaen, F. Sanz-Rodriguez, J. Cuevas, S. Gonzalez, *Clin. Transl. Oncol.* **2008**, *10*, 148–154.
[17] R. Bonnett, *Chemical Aspects of Photodynamic Therapy*, Gordon and Breach Science Publishers, London, **2000**.
[18] R. R. Allison, C. H. Sibata, *Photodiagn. Photodyn. Ther.* **2010**, *7*, 61–75.
[19] F. H. J. Figge, G. S. Weiland, L. O. J. Manganiello, *Proc. Soc. Exp. Biol. Med.* **1948**, *68*, 640–641.
[20] R. Ackroyd, C. Kelty, N. Brown, M. Reed, *Photochem. Photobiol.* **2001**, *74*, 656–669.
[21] F. S. De Rosa, M. V. L. B. Bentley, *Pharm. Res.* **2000**, *17*, 1447–1455.
[22] M. G. H. Vicente, *Curr. Med. Chem. Anti-Cancer Agents* **2001**, *1*, 175–194.
[23] a) C. Lottner, R. Knuechel, G. Bernhardt, H. Brunner, *Cancer Lett.* **2004**, *203*, 171–180; b) C. Lottner, K.-C. Bart, G. Bernhardt, H. Brunner, *J. Med. Chem.* **2002**, *45*, 2064–2078; c) C. Lottner, K.-C. Bart, G. Bernhardt, H. Brunner, *J. Med. Chem.* **2002**, *45*, 2079–2089; d) H. Brunner, K.-M. Schellerer, B. Treittinger, *Inorg. Chim. Acta* **1997**, *264*, 67–79; e) H. Brunner, H. Obermeier, *Angew. Chem. Int. Ed. Engl.* **1994**, *33*, 2214–2215; *Angew. Chem.* **1994**, *106*, 2305–2306.
[24] a) R. Song, Y.-S. Kim, C. O. Lee, Y. S. Sohn, *Tetrahedron Lett.* **2003**, *44*, 1537–1540; b) R. Song, Y.-S. Kim, Y. S. Sohn, *J. Inorg. Biochem.* **2002**, *89*, 83–88.
[25] L. Monsú-Scolaro, C. Donato, M. Castriciano, A. Romeo, R. Romeo, *Inorg. Chim. Acta* **2000**, *300–302*, 978–986.

[26] A. Naik, R. Rubbiani, G. Gasser, B. Spingler, *Angew. Chem. Int. Ed.* **2014**, *53*, 6938 – 6941; *Angew. Chem.* **2014**, *126*, 7058 – 7061.
[27] T. Gianferrara, A. Bergamo, I. Bratsos, B. Milani, C. Spagnul, G. Sava, E. Alessio, *J. Med. Chem.* **2010**, *53*, 4678 – 4690.
[28] F. Schmitt, N. P. E. Barry, L. Juillerat-Jeanneret, B. Therrien, *Bioorg. Med. Chem. Lett.* **2012**, *22*, 178 – 180.
[29] F. Schmitt, P. Govindaswamy, G. Süss-Fink, W. H. Ang, P. J. Dyson, L. Juillerat-Jeanneret, B. Therrien, *J. Med. Chem.* **2008**, *51*, 1811 – 1816.
[30] C. Spagnul, R. Alberto, G. Gasser, S. Ferrari, V. Pierroz, A. Bergamo, T. Gianferrara, E. Alessio, *J. Inorg. Biochem.* **2013**, *122*, 57 – 65.
[31] T. Gianferrara, C. Spagnul, R. Alberto, G. Gasser, S. Ferrari, V. Pierroz, A. Bergamo, E. Alessio, *ChemMedChem* **2014**, *9*, 1231 – 1237.
[32] R. Alberto in *Bioinorganic Medicinal Chemistry* (Ed.: E. Alessio), Wiley-VCH, Weinheim, **2011**, pp. 253 – 282.
[33] A. Leonidova, G. Gasser, *ACS Chem. Biol.* **2014**, *9*, 2180 – 2193.
[34] P. Collery, G. Bastian, F. Santoni, A. Mohsen, M. M. Wei, T. Collery, A. Tomas, D. Desmaele, J. D'Angelo, *Anticancer Res.* **2014**, *34*, 1679 – 1690.
[35] I. Kitanovic, S. Can, H. Alborzinia, A. Kitanovic, V. Pierroz, A. Leonidova, A. Pinto, R. Molteni, B. Spingler, S. Ferrari, A. Steffen, N. Metzler-Nolte, S. Wölfl, G. Gasser, *Chem. Eur. J.* **2014**, *20*, 2496 – 2507.
[36] a) R. J. J. Fiel, *J. Biomol. Struct. Dyn.* **1989**, *6*, 1259 – 1274; b) R. F. Pasternack, E. J. Gibbs, *Met. Ions Biol. Syst.* **1996**, *33*, 367 – 397; c) G. Pratviel, J. Bernadou, B. Meunier, *Met. Ions Biol. Syst.* **1996**, *33*, 399 – 426; d) L. G. Marzilli, *New J. Chem.* **1990**, *14*, 409 – 420.
[37] a) R. Fiel, B. Jenkins, J. Alderfer in *The 23rd Jerusalem Symposium in Quantum Chemistry and Biochemistry, Vol. 23* (Eds.: B. Pullman, J. Jortner), Kluwer Academic Publishers, Netherlands, **1990**, pp. 385 – 399; b) R. J. Fiel, N. Datta-Gupta, E. H. Mark, J. C. Howard, *Cancer Res.* **1981**, *41*, 3543 – 3545.
[38] a) H. Han, D. R. Langley, A. Rangan, L. H. Hurley, *J. Am. Chem. Soc.* **2001**, *123*, 8902 – 8913; b) J. Seenisamy, S. Bashyam, V. Gokhale, H. Vankayalapati, D. Sun, A. Siddiqui-Jain, N. Streiner, K. Shin-Ya, E. White, W. D. Wilson, L. H. Hurley, *J. Am. Chem. Soc.* **2005**, *127*, 2944 – 2959.
[39] a) L. Martino, B. Pagano, I. Fotticchia, S. Neidle, C. J. Giancola, *J. Phys. Chem. B* **2009**, *113*, 14779 – 14786; b) A. Cummaro, I. Fotticchia, M. Franceschin, C. Giancola, L. Petraccone, *Biochimie* **2011**, *93*, 1392 – 1400.
[40] a) I. M. Dixon, F. Lopez, A. M. Tejera, J. P. Estève, M. A. Blasco, G. Pratviel, *J. Am. Chem. Soc.* **2007**, *129*, 1502 – 1503; b) C. Romera, O. Bombarde, R. Bonnet, D. Gomez, P. Dumy, P. Calsou, J. F. Gwan, J. H. Lin, E. Defrancq, G. Pratviel, *Biochimie* **2011**, *93*, 1310 – 1317.
[41] a) D. F. Shi, R. T. Wheelhouse, D. Sun, L. H. Hurley, *J. Med. Chem.* **2001**, *44*, 4509 – 4523; b) E. P. Cohn, K. L. Wu, T. R. Pettus, N. O. Reich, *J. Med. Chem.* **2012**, *55*, 3678 – 3686.
[42] a) A. Siddiqui-Jain, C. L. Grand, D. J. Bearss, L. H. Hurley, *Proc. Natl. Acad. Sci. USA* **2002**, *99*, 11593 – 11598; b) C. L. Grand, H. Han, R. M. Muñoz, S. Weitman, D. D. Von Hoff, L. H. Hurley, D. J. Bearss, *Mol. Cancer Ther.* **2002**, *1*, 565 – 573.
[43] I. M. Dixon, F. Lopez, J.-P. Esteve, A. M. Tejera, M. A. Blasco, G. Pratviel, B. Meunier, *ChemBioChem* **2005**, *6*, 123 – 132.
[44] a) S. Balasubramanian, S. Neidle, *Curr. Opin. Chem. Biol.* **2009**, *13*, 345 – 353; b) S. Balasubramanian, L. H. Hurley, S. Neidle, *Nat. Rev. Drug Discovery* **2011**, *10*, 261 – 275; c) G. W. Collie, G. N. Parkinson, *Chem. Soc. Rev.* **2011**, *40*, 5867 – 5892; d) M. Düchler, *J. Drug Targeting* **2012**, *20*, 389 – 400.
[45] a) T. B. Krystona, A. B. Georgieva, P. Pissis, A. G. Georgakilas, *Mutation Res.* **2011**, *711*, 193 – 201; b) R. De Bont, N. van Larebeke, *Mutagenesis* **2004**, *19*, 169 – 185.
[46] R. Alberto, W. A. Herrmann, P. Kiprof, F. Baumgartner, *Inorg. Chem.* **1992**, *31*, 895 – 899.
[47] H. Braband, S. Imstepf, M. Benz, B. Spingler, R. Alberto, *Inorg. Chem.* **2012**, *51*, 4051 – 4057.
[48] C. Pomp, S. Drüeke, H. J. Küppers, K. Wieghardt, C. Kruger, B. Nuber, J. Weiss, *Z. Naturforsch. B* **1988**, *43*, 299 – 305.
[49] a) A. C. Benniston, P. Gunning, R. D. Peacock, *J. Org. Chem.* **2005**, *70*, 115 – 130; b) S. Kimura, E. Bill, E. Bothe, T. Weyhermuller, K. Wieghardt, *J. Am. Chem. Soc.* **2001**, *123*, 6025 – 6039.
[50] T. Gianferrara, I. Bratsos, E. Iengo, B. Milani, A. Oštrić, C. Spagnul, E. Zangrando, E. Alessio, *Dalton Trans.* **2009**, 10742 – 10756.
[51] F. Schmitt, P. Govindaswamy, O. Zava, G. Süss-Fink, L. Juillerat-Jeanneret, B. Therrien, *J. Biol. Inorg. Chem.* **2009**, *14*, 101 – 109.
[52] K. Davia, D. King, Y. Hong, S. Swavey, *Inorg. Chem. Commun.* **2008**, *11*, 584 – 586.
[53] a) C.-T. Poon, P.-S. Chan, C. Man, F.-L. Jiang, R. N. S. Wong, N.-K. Mak, D. W. J. Kwong, S.-W. Tsao, W.-K. Wong, *J. Inorg. Biochem.* **2010**, *104*, 62 – 70; b) J.-X. Zhang, J.-W. Zhou, C.-F. Chan, T. C.-K. Lau, D. W. J. Kwong, H.-L. Tam, N.-K. Mak, K.-L. Wong, W.-K. Wong, *Bioconjugate Chem.* **2012**, *23*, 1623 – 1638.
[54] E. Delaey, F. van Laar, D. De Vos, A. Kamuhabwa, P. Jacobs, P. A. de Witte, *J. Photochem. Photobiol. B* **2000**, *55*, 27 – 36.
[55] M. Ochsner, *J. Photochem. Photobiol. B* **1997**, *39*, 1 – 18.
[56] a) B. M. Sutherland, P. V. Bennett, M. Saparbaev, J. C. Sutherland, J. Laval, *Radiat. Prot. Dosim.* **2001**, *97*, 33 – 38; b) S. Britz-Cunningham, S. Adelstein, *J. Nucl. Med.* **2003**, *44*, 1945 – 1961; c) M. Hada, A. G. Georgakilas, *J. Radiat. Res.* **2008**, *49*, 203 – 210; d) N. Shikazono, M. Noguchi, K. Fujii, A. Urushibara, A. Yokoya, *J. Radiat. Res.* **2009**, *50*, 27 – 36.
[57] a) A. I. Kassis, *J. Nucl. Med.* **2003**, *44*, 1479 – 1481; b) M. L. Schipper, C. G. U. Riese, S. Seitz, A. Weber, M. Behe, T. Schurrat, N. Schramm, B. Keil, H. Alfke, T. M. Behr, *Eur. J. Nucl. Med. Mol. Imaging* **2007**, *34*, 638 – 650; c) A. A. S. Tavares, J. M. R. S. Tavares, *Int. J. Radiat. Biol.* **2010**, *86*, 261 – 270.
[58] T. Esteves, C. Xavier, S. Gama, F. Mendes, P. D. Raposinho, F. Marques, A. Paulo, J. Costa Pessoa, J. Rino, G. Viola, I. Santos, *Org. Biomol. Chem.* **2010**, *8*, 4104 – 4116.
[59] a) R. G. Balasingham, M. P. Coogan, F. L. Thorp-Greenwood, *Dalton Trans.* **2011**, *40*, 11663 – 11674; b) F. L. Thorp-Greenwood, M. P. Coogan, L. Mishra, N. Kumari, G. Raic, S. Saripella, *New J. Chem.* **2012**, *36*, 64 – 72; c) V. Fernández-Moreira, F. L. Thorp-Greenwood, A. J. Amoroso, J. Cable, J. B. Court, V. Gray, A. J. Hayes, R. L. Jenkins, B. M. Kariuki, D. Lloyd, C. O. Millet, C. Ff. Williams, M. P. Coogan, *Org. Biomol. Chem.* **2010**, *8*, 3888 – 3901.
[60] M. Casanova, E. Zangrando, F. Munini, E. Iengo, E. Alessio, *Dalton Trans.* **2006**, 5033 – 5045.
[61] P. D. Beer, J. Cadman, J. M. Lloris, R. Martínez-Máñez, J. Soto, T. Pardo, M. D. Marcos, *J. Chem. Soc. Dalton Trans.* **2000**, 1805 – 1812.
[62] M. C. Alley, D. A. Scudiero, A. Monks, M. L. Hursey, M. J. Czerwinski, D. L. Fine, B. J. Abbott, J. G. Mayo, R. H. Schoemaker, M. R. Boyd, *Cancer Res.* **1988**, *48*, 589 – 601.
[63] C. Mari, V. Pierroz, R. Rubbiani, M. Patra, J. Hess, B. Spingler, L. Oehninger, J. Schur, I. Ott, L. Salassa, S. Ferrari, G. Gasser, *Chem. Eur. J.* **2014**, *20*, 14421 – 14436.

Received: July 3, 2015
Revised: August 13, 2015
Published online on September 2, 2015